



## RESEARCH ON DEVELOPMENT AND ANALYSIS OF DEEP LEARNING MODELS FOR LUNG CANCER DIAGNOSIS IN HISTOPATHOLOGICAL IMAGES

Jayant Bokefode<sup>1\*</sup>, Dr. MV Panduranga Rao<sup>2</sup>, Dr. Komarasamy G<sup>3</sup>

### Abstract:

Lung cancer is the most diagnosed cancer after breast cancer. Computed Tomography (C.T.) scan is the most used imaging technique in the medical field to diagnosis lung cancer. Still, it is difficult to infer and not identify benign and malignant nodules based on imaging tests. In such cases, doctors advise or recommend lung biopsy. Manual pathological detection systems are a time-consuming, tedious, exhausting task and may lead to medical error; hence computer-aided diagnosis is preferred to obtain better results. In this work, we have collected data of 97 patient records that did a lung biopsy. First, images are prepared using histopathology. Next, stain normalization, image processing techniques, and data augmentation are applied to prepare the dataset. This research work demonstrates an approach to designing and training various variants of the Convolutional neural network to diagnose Lung Cancer in histopathological images.

**Keywords:** Lung Cancer, Histopathological images, Deep Learning, Convolutional Neural Networks, Variants of CNN

---

<sup>1\*</sup>Department of Computer Science Engineering, School of Engineering and Technology, JAIN (Deemed-To-Be-University), Bangalore - 562 112. E-mail: bokefode.jayant@gmail.com

<sup>2</sup>Department of CSE/ISE, School of Engineering and Technology, JAIN (Deemed-To-Be-University), Bangalore - 562 112. E-mail: raomvp@yahoo.com

<sup>3</sup>School of Computing Science & Engineering, VIT Bhopal University, Madhya Pradesh - 4661144, India. E-mail: gkomarasamy@gmail.com

**\*Corresponding Author:** Jayant Bokefode

\*Department of Computer Science Engineering, School of Engineering and Technology, JAIN (Deemed-To-Be-University), Bangalore - 562 112. E-mail: bokefode.jayant@gmail.com

**DOI:** - 10.31838/ecb/2023.12.si5.0116

## 1 Introduction

As per World Lung Cancer Day, 2020 Fact Sheet published by the American College of Chest Physicians, lung cancer is the most diagnosed cancer (11.6%) after breast (11.6%) and colorectal cancers (10.2%) [1]. The mortality rate of lung cancer surpasses breast cancer, and by 2030 it is estimated to reach 2.45 million worldwide. As per the various studies, 80% of lung cancer deaths are due to smoking tobacco [1]. Doctors and health workers are adopting different health informatics techniques to improve healthcare services and ease the diagnosis process. Scientists are working and developing computer-aided diagnosis systems to relieve the efforts of doctors. It also speeds up the examination and reduces medical costs.

Nowadays, many researchers are developing machine learning models to diagnosis various types of diseases [2-4]. However, developed machine learning models fail to predict correct diagnosis on unseen data due to various reasons. Accurate disease diagnosis and patient monitoring through-out recovery are essential and don't have any medical errors because they may lead to death. As per the recent study by Hopkins, approximately 250,000 people in the U.S. die every year due to medical errors [5]. Other reports claim that up to 440,000 people die due to medical errors and lack of specialists, which is the third primary cause of death. Another study published by Harvard University last year mentions that around 500,000 deaths per year are happened in India due to medical errors and lack of practical knowledge among the doctors. Therefore, almost 100 percent accuracy is necessary for health care systems. By 2030 India require around 20 lakh doctors to satisfy the norms specified by WHO's standard that is 1:1000 [5]. Rural Health Statistics (RHS) 2017 states that there are a lack of 87% surgeons, 74% Gynecologists & Obstetricians, 85% Physicians, and 81% Pediatricians in the CHCs in rural India[6-7].

Computed Tomography (C.T.) scan is the most used imaging technique in the medical field to diagnosis lung cancer [8-9]. Still, sometimes it is difficult for doctors to infer and categorize cancer. In some cases, doctors are not able to identify benign and malignant nodules based on imaging tests. In such cases, doctors advise or recommend for biopsy [10]. The lung biopsy follows imaging guidance to collect the lung tissue sample to examine under a microscope. Images are captured and prepared using histopathology; it includes the affected tissue's biopsy [11-13]. The pathologist extracts the affected tissues from the tumour and stains them with H& E (hematoxylin and eosin). These are then scanned under a microscope to determine malignant features such as nuclei to identify cancerous cells [14]. Manual examination of the cancerous cell is a time-consuming, tedious, exhausting task and may lead to medical error [15]. Therefore, histopathological images are collected and categorized into normal and cancerous and used to develop an advanced computerized system to diagnosis lung cancer.

Researchers are developing and implementing various image processing and machine learning techniques to develop computer-aided diagnosis systems [16]. Machine Learning model is not efficient and effective as compared to the Deep Learning models sometimes. It also fails to predict the correct class for unseen data on image datasets for various reasons [17]. Machine learning models are simple and deal with a small set of features. Firstly we need to extract the features from the images to train the machine learning model. Then, we have to use various image processing techniques. Extracting features from images is a very complicated and time-consuming task, and we are not sure that extracted features were able to predict the correct class. But the deep learning networks do not necessarily need structured/labelled data of the images. Some deep learning networks calculate image features very effectively; it will save the efforts required to extract the features manually from the images [18]. This research aims to evaluate the various computer-aided techniques, analyse the current best process, find out their limitations and drawbacks, and propose a new model with improvements in the current best model.

2 Why Deep Learning?

## 2 Why Deep Learning?

Machine learning is a subsection of Artificial Intelligence; similarly, deep learning is also considered a subset of machine learning. Deep learning is derived from artificial neural networks to emulate how the human brain processes the data to identify any object. The brain has a network of neurons which take all kind of inputs like visuals, sensation and so on and process it [28]. The Convolutional neural network is also known as ConvNets or CNNs, one of the primary and widely used neural network techniques. It has various computer vision applications like image classifications, video recognition, object detections, recommendation, and natural language processing [29-30]. CNN is also made up of neurons that take inputs, calculate weighted sum, pass them to the activation function, and respond with an output[31-32]. Over the last few years, various variants of CNN architecture is developed and published, and these variants give remarkable results in the field of deep learning [33]. This research work demonstrates an approach to designing and training various variants of the Convolutional neural network

to diagnose Lung Cancer in histopathological images.

### 3 Methodology

#### 3.1 Network Architecture

Figure 1 depicts a block diagram of the proposed methodology for this research. Lung biopsy samples are collected and images are created out of them. The visual information of each input image has been improved by using pre-processing strategies. Different data techniques are responsible for increment in the size of training dataset.

Such prepared input images are fed into the Convolutional layer. The convolutional layer creates feature maps. The noise and dimensions of such feature maps are reduced using max pooling. The pooled feature map is then flattened and used as input to the fully connected layer as a one-dimensional array. The model is continuously trained over a sequence of epochs. The trained model can perceive low-level features in images, distinguish between the dominant segments, and classify them using sigmoid classification. Table 1 lists the parameters of the built CNN network.

#### 3.2 Dataset Preparation

##### 3.2.1 Image augmentation:

Deep learning techniques require a vast amount of data for learning [19]. Therefore, training the CNN

with limited samples may lead to over fitting and less accuracy in prediction. Image augmentation is the one way to avoid this issue [20]. Application of different image augmentation techniques like zooming, flipping, rotation, shifting, blurring can generate more training samples [20-21].

Use of Shearing range, zooming, and horizontal flipping to increase the collected dataset to train CNN and its variants is applied in the process. Before applying image augmentation, the background of all the samples is cleaned and all samples are arranged in the same size and resolution, i.e.640\*480 and 3 respectively. The plot of the augmented sample is displayed in Fig.2.

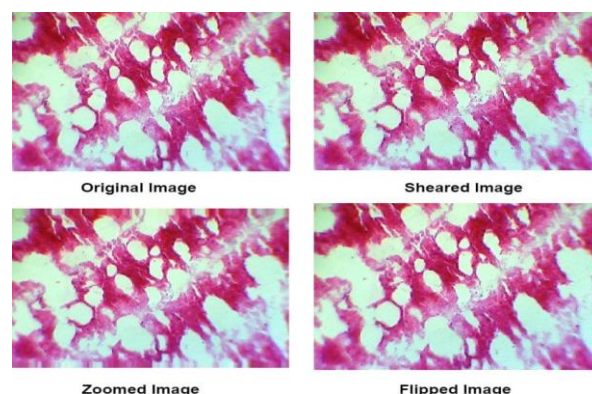


Fig.2. Augmented Images

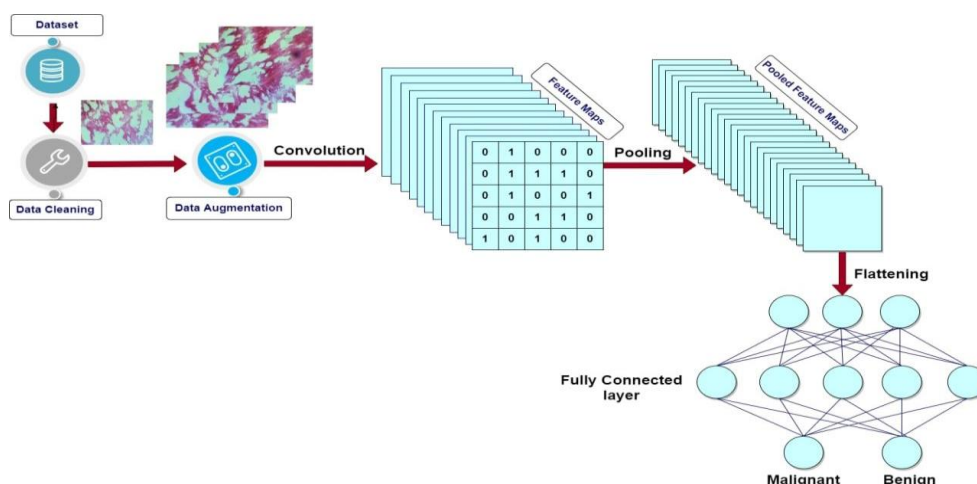


Fig.1. Proposed CNN architecture for lung diagnosis.

Table 1 Parameters of the CNN architecture developed for Lung Cancer Diagnosis.

Layer attribute	L1	L2	L3	L4	L5	L6	L7	L8	L9	L10
Type	Conv	Pool	Conv	Pool	Conv	Pool	Conv	Pool	Conv	Pool
Channel	32	-	32	-	32	-	32	-	64	-
Filter Size	3×3	-	3×3	-	3×3	-	3×3	-	3×3	-
Conv. Stride	1×1	-	1×1	-	1×1	-	1×1	-	1×1	-
Pooling Size	-	2×2	-	2×2	-	2×2	-	2×2	-	2×2
Pooling Stride	-	1×1	-	1×1	-	1×1	-	1×1	-	1×1
Padding Size	same	none	-	none	-	none	-	none	-	none
Activation	Relu	-	Relu	-	Relu	-	Relu	-	Relu	-

### 3.2.2 Stain Normalization:

The pathologist extracts the affected tissues from the tumour and stains them with H& E (hematoxylin and eosin) to determine the differences between nuclei stained with purple color and remaining structure stained with pink and red color[14][21]. The collected tissues are stained to analyze the shape, density, and variability of nuclei and the complete structure of tissues. However, while H & E staining different protocols, scanners, and raw materials are getting used, this leads to variability between collected images [22-24]. Therefore, the stain-normalization of

H&E stained histology slides is necessary to reduce the color variation. It helps obtain a better color consistency before feeding input images into the proposed architecture. We have used Macenko et al. [25] approach for stain normalization because of its promising results. Macenko's method is established on a singular value decomposition (SVD) standardizing the tissue's color intensity. In addition, Macenko's approach uses a logarithmic function [26] which adaptively transfers color concentration into its optical density (O.D.) as given in equation 1.

$$OD = -\log(I/I_0) \quad (1)$$

I is the image intensity in RGB space, and I<sub>0</sub> is the illuminating intensity incident on the histological sample.

### 3.3 Proposed CNN architecture

Image is nothing but a binary representation of visual data. It is a matrix of pixels arranged like a grid, and each pixel has a value that denotes a color and its brightness. CNN is widely used and specialized in processing a vast amount of data stored in a grid-like structure such as an image. A CNN mainly has three layers: a convolutional layer, a pooling layer, and a fully connected layer [30][31]. CNN is a feed-forward neural network that operates over the volumes. CNN takes a multi-channeled image as an input, whereas a neural network takes a vector. The input data to the CNN model will look like the following picture. The CNN takes a 4D array as input, and it has a shape of (batch\_size, height, width, depth) shown in Fig.3 [34]. Depth represents the number of color channels presents in the image. The depth size in the RGB image would be three, and for the gray scale image, it would be one. The given input to CNN goes to various layers, and it generates an output of a 4D array. The image dimensions may vary based on filters, kernel size, and padding. The

batch size would be the same as the input batch size.

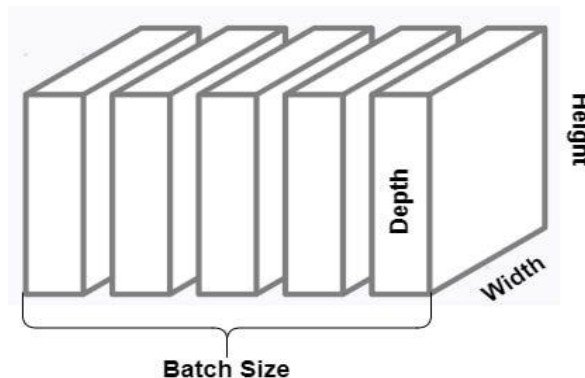


Fig.3. CNN Input Shape

#### 3.3.1 Convolution layer

Convolution is the mathematical operation that involves the multiplication of the feature detector (filter) and the input image. The feature detector is smaller than the input matrix, and the dot product is calculated by sliding it on the input array. Ideally, the feature detector is a 3\*3 matrix. The filter slides across the image left to right, top to bottom pixel by pixel; this movement is called stride. The default stride is (1, 1). A single value is obtained by multiplying the filter and the input array once. The filter is applied several times to the input array, resulting in a two-dimensional array. The resulted in a two-dimensional array from a multiplication operation called a feature map. Using different filters to an input image can perform operations like edge detection, blur, and sharpening. Each value from the resulted feature map is going through nonlinearity [30-31].

ReLU is an activation function applied to each value in the feature map to reduce the image nonlinearities [35]. After rectifying an image, the progression from one color to the other is more abrupt instead of gradual. In the proposed CNN architecture, five convolution layers are added along with the ReLU activation function. The first convolution layer has 32 filter-sizes, 3\*3 kernel-size, and input shape is 256\*256\*3. The last Convolution layer has 64 filter-sizes and 3\*3 kernel-size. Fig 4 depicts the steps involved in a convolutional layer.

#### 3.3.2 Pooling and Flattening Layer

The pooling layer plays a similar role to the convolution layer. It reduces the spatial size of a convolved feature. Dimensionality reduction is helpful to decrease the computational power required to process the vast amount of data.

The polling layer extracts the dominant features from the feature map that effectively train the model. Max polling reduces the noise from the im-



age along with dimensionality reduction. It also helps to reduce over fitting. In the proposed model, max pooling is added with pool-size (2, 2). One can add as many layers by combining the convolution layers and the pooling layer depending upon the image complexities. However, adding too many layers may increase the cost of computational power. After pooling, the next step in the Convolutional neural network is flattening. Flattening converts the pooled feature map into a one-dimensional array. The resulting column vector is input to the fully connected layer [30-31]. It is graphically represented in Fig. 5.

#### 4 Variants of CNN

Convolutional neural networks (ConvNets) are the most successful and incredible advances in large-scale image and video recognition[36-38]. Researchers and developers introduced different variants of CNN's by using ImageNet database and high-performance computing systems, such as GPUs or large-scale distributed clusters [39][40], and it is getting deeper and deeper. ImageNet played an essential role in the advancement of the CNN model by providing large open-source image repositories. ImageNet also hosts an annual competition named ImageNet Large Scale Visual Recognition Challenge (ILSVRC) for researchers and developers to present their developed architecture every year [41]. Different variants of CNNs have been implemented on histopathological images

to diagnose lung cancer. This is most successful, and secured a top position in this competition like VGG16, VGG19, ResNet50, and InceptionV3. Their performances in terms of accuracy and loss value have been compared later.

#### 4.1 VGG16 and VGG19

The VGG16 and VGG19 were invented by the Visual Geometry Group (VGG), and these are runner-up of the ILSVRC-2014 competition. Simonyan and Zisserman designed VGG16 has 13 convolutional layers with filters size 3×3 and stride=1 followed by a max-pooling layer with filters size 2×2 and stride=2 and 3 fully-connected layers, carrying with them the ReLU. It achieved a top-5 error rate of 5.1%. VGG is frequently used and preferred for feature extraction from the images because the weight configuration of the VGG Net is open-source. Therefore, it is helpful in many applications and challenges as a feature extractor. However, it consists of around 138 million parameters which can be challenging to handle [42]. The VGG16 and VGG19 models have been created and trained on histopathological images of lungs. Table 2 shows the structured details of the VGG16 and VGG19 model.

#### 4.2 ResNet50

Res Net Stood for Residual Networks and was invented by Kaiming He et al. and the ILSVRC 2015 challenge winner.

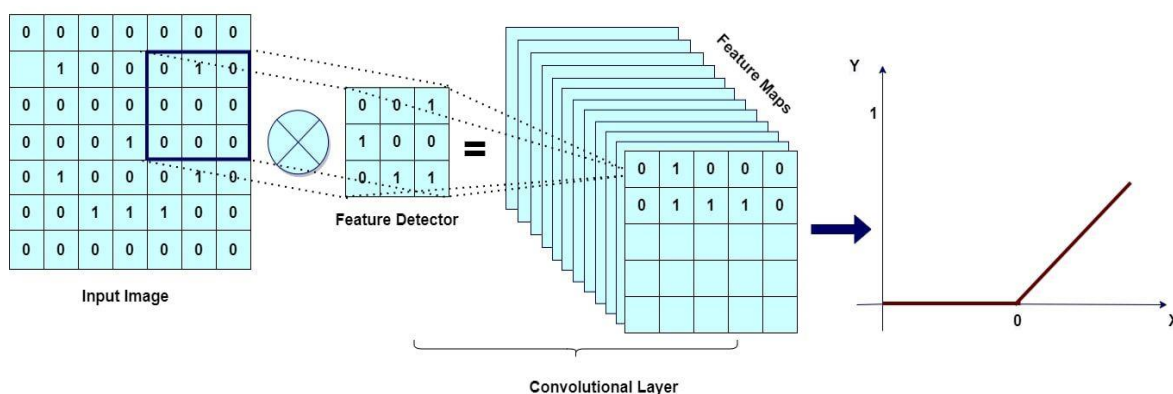


Fig.4. CNN Convolutional layer steps.

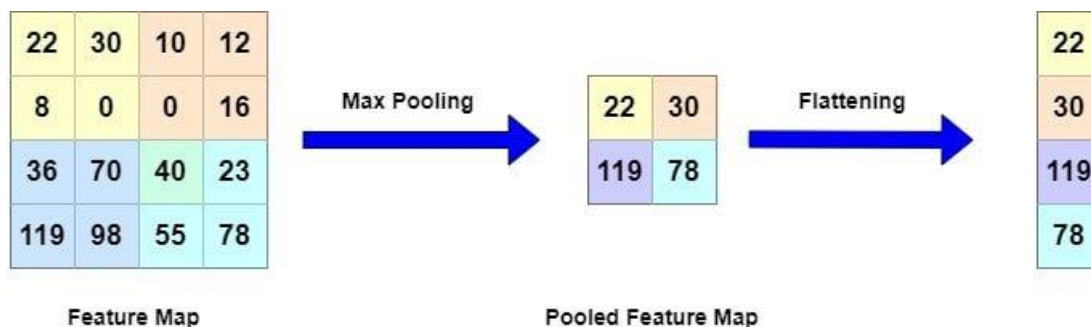


Fig 5: CNN Max Pooling and flattening layer.

Deeper neural networks are complex to train, and they require high computing power. Training deeper networks results in degradation of performance over the long run and faces a vanishing and exploding gradient type of problem. In vanishing gradient, recurrent multiplication being done, because the gradient is being back-propagated, makes the gradient infinitely little [43-44].

The ResNet architecture has 152 layers which are 8x more profound than the VGG network. Nevertheless, it achieved a top-5 error rate of 3.6%, with lower complexity than AlexNet and VGG on the ImageNet dataset. This is because of ResNet has a residual block, designed based on skip connections and heavy batch normalization. Skip connections allow you to activate one layer and suddenly feed it to another layer even much deeper in the neural network. When we create a neural network, initially, its weights are close to zero; therefore, network output also close to zero. If we add a skip connection, the resulting network outputs a copy of its inputs, and it improves the speed of training considerably [43-44]. The identity function is easy for the residual block to learn, and it's easy to get  $a[l+2]$  that equals  $a[l]$  because of this skip connection (1 – layer, a – activation). The residual learning block mechanism is explained in Fig. 6

**Table 2** Structured details of VGG16 and VGG19 model

Layer(Type)	VGG16	VGG19
No. of Weight Layers	16	19
Input Shape	(244, 244, 3)	(244, 244, 3)
Convolution layers	13	16
Filter Size	3×3	3×3
ReLU	5	18
Max Pooling layers	5	5
Fully Connected layer	2	2
Optimizer	RMSprop	Adam

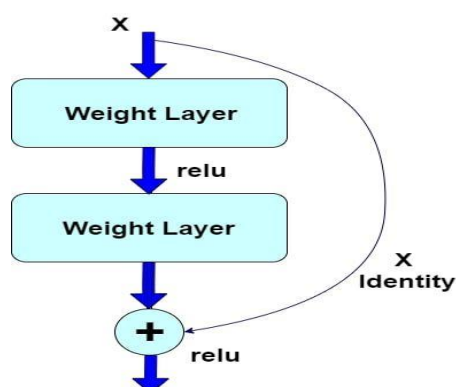


**Fig.6.** Skip Connection mechanism.

### 4.3 Inception-V3

Inception –v3 is also a variant of convolutional neural network architecture from the inception family and was developed by Google, and it achieved a top -5 error rate of 6.67%. It is a winner Eur. Chem. Bull. 2023, 12(Special Issue 5), 962 – 971

of the ILSVRC 2014 competition. The existing inception models are refined by introducing various techniques like Label Smoothing, using an auxiliary classifier to transmit label details to the lower down the network, batch normalization, and factorized  $7 \times 7$  convolutions [45]. The basic idea behind the inception model is that, rather than implementing convolutional layers of varied hyper parameters in numerous layers, one tend to do all the convolution together and output a result containing matrices from all the filter operations together The motivation behind this model is to reduce the input dimensions of the next layer and efficient computation by using factorization [45-46]. The inception model consists of several models called inception modules. Each model will perform four functions parallelly first  $1 \times 1$  convolution layer, followed by a  $3 \times 3$  convolution layer, then a  $5 \times 5$  convolution layer, and at last, max pooling. Inception 3 has 11 inception modules; global average pooling is used at the end of the last inception modules [47-48].

The Inception-v3 model is implemented to diagnose Lung Cancer in histopathological images by using the Keras library. Table 3 shows the structured details of the Inception-V3 model.

**Table 3** Structured details of Inception-V3

Layer(Type)	Inception-V3
Modules	11 inception modules
Input Shape	(244, 244, 3)
Convolution layers	48
Filter Size	(1x1, 3x3, 5x5)
Activation Function (Conv)	ReLU
Max Pooling Size	3x3
Fully Connected layer	2
Drop Out	0.5
Optimizer	Adam
Batch Size	50
Activation Function (FCL-1)	ReLU
Activation Function (FCL-2)	Sigmoid

### 4 Experimental Results and Discussion

This research paper mainly focuses on the classification of the histopathological image of lungs into malignant and benign. Model accuracy and loss are determined to evaluate the effectiveness of the CNN model and its variants. The loss is in negative log-likelihood in neural networks; therefore, the learning objective is to minimize the loss function value in respect of model parameters by changing the weight values by optimizing it with different techniques like back propagation. Loss value indicates how a model will behave after each epoch. Ideally, we should train the model so that the model Loss value will be minimum after each or several iterations. If the model loss is lower, that means the model is suitable to predict the expected

results. The model loss is calculated on the training and validation set, and it's not in a percentage. Instead, it is an addition to the errors made for each sample in training or validation sets. The model accuracy is calculated based on the correct classification done by the model. After completing training, test samples are fed to the model; if the model classifies 95 samples correctly out of 100, the model accuracy is 95 %.

Training and testing set are created by dividing images into 80 and 20, respectively. The developed CNN model has given 94.40% training accuracy and 89.58% validation accuracy after 48 epochs.. The validation loss is greater than training loss that means the model is not overfitting. CNN model training loss is 0.1680%, and validation loss is 0.3305%. Similarly, we have developed and trained VGG16, VGG19, ResNet50, and Inception-v3 models. VGG16 and VGG19 models have provided training accuracy 100 and validation accuracy 77.66% after 11 epochs and 79.69% after 84 epochs. A VGG16 and VGG19 model training loss is 0.0010% and 0.0013%, and validation loss is 0.8004% and 0.7192% after 11 epochs and 84 epochs. We observed VGG16 is started overfitting after 11 epochs and VGG19 after 84 epochs. Res-Net50 model has given training accuracy 100% with a loss of 0.0303%, and validation accuracy is 91.15% with a loss of 0.2284% after 84 epochs. Inception-v3 has given training accuracy 94.34% with a loss of 0.1644%, and validation accuracy is 86.46% with a loss of 0.3432% after 20 epochs.

### 5 Conclusion and future scope

This paper presents a deep learning approach for the diagnosis of lung cancer from histopathology images. We implemented well-established CNNs architecture and its variants, namely VGG-16, VGG19, ResNet50, and Inception-V3. By changing the network design and characteristics, we may be able to achieve better outcomes. The comparative analysis of implemented deep learning models is shown in table no.5 and model accuracies of all implemented models are graphically represented in Fig.7 to Fig.11 respectively. Furthermore, compared to single classifiers, the combination of CNN models results in more incredible generalization performance. This study will serve as the foundation for a future paper on deep learning integration. In future work CNN, ResNet50 and Inception-v3 will be combined together by using ensemble machine learning models to achieve better prediction accuracy on unseen data.

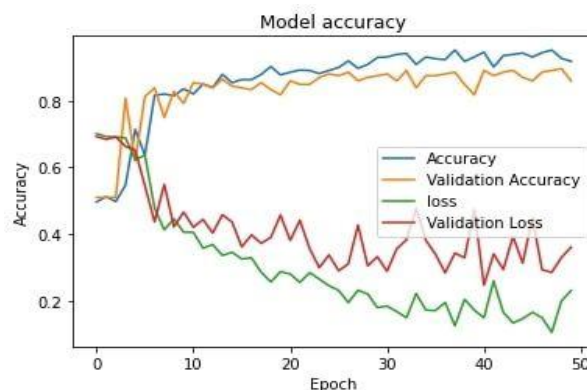


Fig. 7. CNN training and validation accuracy and loss

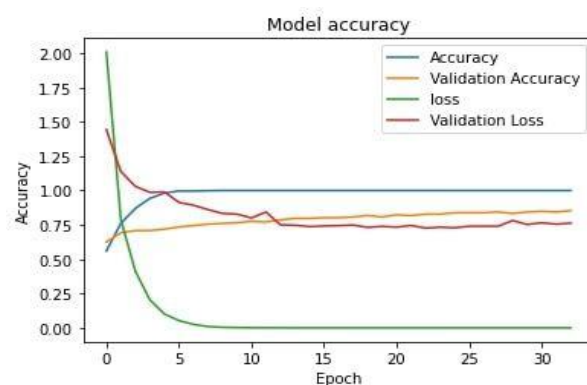


Fig.8. VGG16 training and validation accuracy and loss

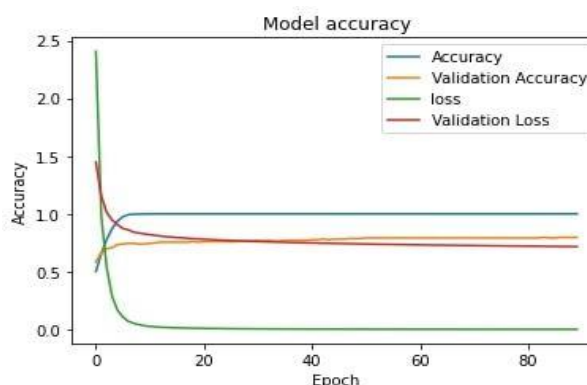


Fig.9. VGG19 training and validation accuracy and loss

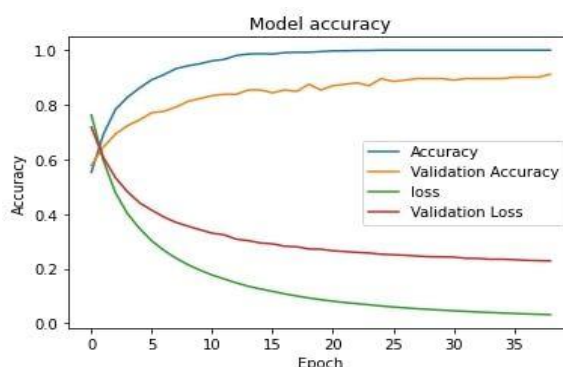
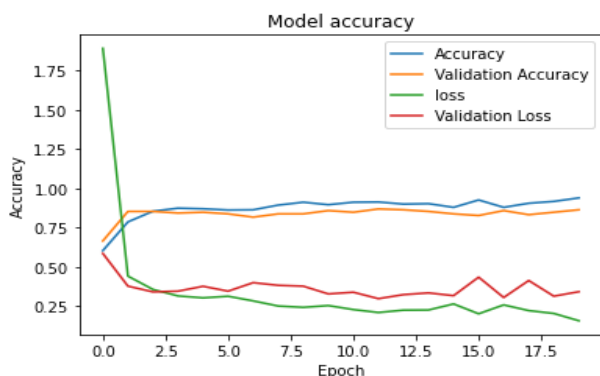


Fig.10. ResNet50 training and validation accuracy and loss



**Fig.11.** Inception-V3 training and validation accuracy and loss

**Table 5** Comparative analysis of implemented deep learning models.

Implemented Networks	Number of epochs	Batch Size	Training Accuracy	Validation Accuracy	Training loss	Validation Loss
CNN	48	20	94.4	89.58	0.168	0.3305
VGG16	11	50	100	77.66	0.001	0.8004
VGG19	84	50	100	79.69	0.0013	0.7192
ResNet50	39	50	100	91.15	0.0303	0.2284
Inception-V3	20	50	94.34	86.46	0.1644	0.3432

**References**

- World Lung Cancer Day 2020 Fact, <https://www.chestnet.org/News/CHEST-News/2020/07/World-Lung-Cancer-Day-2020-Fact-Sheet>. July 31, 2020.
- Corbett, E., The Real-World Benefits of Machine Learning in Healthcare. April 25, 2017, <https://www.healthcatalyst.com/clinical-applications-of-machine-learning-in-healthcare>.
- Fatima, M. and Pasha, M. (2017) Survey of Machine Learning Algorithms for Disease Diagnostic. *Journal of Intelligent Learning Systems and Applications*, 9, 1-16. doi: 10.4236/jilsa.2017.91001.
- Cardoso, I., et al., Analysis of Machine Learning Algorithms for Diagnosis of Diffuse Lung Diseases. *Methods Inf Med*, 2018. 57(5-06): p. 272-279.
- Vanessa McMains. Johns Hopkins study suggests medical errors are third-leading cause of death in U.S. May 4, 2016, <https://hub.jhu.edu/2016/05/03/medical-errors-third-leading-cause-of-death/>[6] Sagi, O, Rokach, L. Ensemble learning: A survey. *WIREs Data Mining Knowl Discov*. 2018; 8:e1249.
- K. Triantafyllidis, et al., Framework of sensor-based monitoring for pervasive patient care. *Healthcare Technology Letters*, 2016. 3(3): p. 153-158.
- Purandare, Nilendu & Rangarajan, Venkatesh. (2015). Imaging of lung cancer: Implications on staging and management. *Indian Journal of Radiology and Imaging*. 25. 109. 10.4103/0971-3026.155831
- Bach, Peter & Mirkin, Joshua & Oliver, Thomas & Azzoli, Christopher & Berry, Donald & Brawley, Otis & Byers, Tim & Colditz, Graham & Gould, Michael & Jett, James & Sabichi, Anita & Smith-Bindman, Rebecca & Wood, Douglas & Qaseem, Amir & Detterbeck, Frank. (2012). Benefits and Harms of CT Screening for Lung Cancer A Systematic Review. *JAMA : the journal of the American Medical Association*. 307. 2418-29. 10.1001/jama.2012.5521.
- Ofiara LM, Navasakulpong A, Ezer N, Gonzalez AV. The importance of a satisfactory biopsy for the diagnosis of lung cancer in the era of personalized treatment. *Curr Oncol*. 2012;19 (Suppl1):S16-S23. doi:10.3747/co.19.1062.
- Tuzi A, Bolzacchini E, Suter MB, et al. Biopsy and re-biopsy in lung cancer: the oncologist requests and the role of endobronchial ultrasounds transbronchial needle aspiration. *J Thorac Dis*. 2017;9(Suppl 5):S405-S409. doi:10.21037/jtd.2017.04.09
- C. de Margerie-Mellon, C. de Bazelaire, E. de Kerviler, Image-guided biopsy in primary lung cancer: Why, when and how, *Diagnostic and Interventional Imaging*, Volume 97, Issue 10, 2016, Pages 965-972, ISSN 2211-5684, <https://doi.org/10.1016/j.diii.2016.06.016>.
- Wagnetz, Ute & Menezes, Ravi & Boerner, Scott & Paul, Narinder & Wagnetz, Dirk & Keshavjee, Shaf & Roberts, Heidi. (2012). CT Screening for Lung Cancer: Implication of Lung Biopsy Recommendations. *AJR. American*



- can journal of roentgenology. 198. 351-8. 10.2214/AJR.11.6726.
13. Fischer AH, Jacobson KA, Rose J, Zeller R. Hematoxylin and eosin staining of tissue and cell sections. CSH Protoc. 2008 May 1; 2008: pdb. prot 4986. doi: 10.1101/pdb.prot4986. PMID: 21356829.
  14. Aksac, A., Demetrick, D.J., Ozyer, T. et al. BreCaHAD: a dataset for breast cancer histopathological annotation and diagnosis. BMC Res Notes 12, 82 (2019). <https://doi.org/10.1186/s13104-019-4121-7>
  15. Suzuki, Kenji. (2013). Machine Learning in Computer-Aided Diagnosis of the Thorax and Colon in CT: A Survey. IEICE transactions on information and systems. E96-D. 772-783. 10.1587/transinf.E96.D.772.
  16. Sejnowski, Terrence. (2020). The Unreasonable Effectiveness of Deep Learning in Artificial Intelligence. PNAS December 1, 2020 117 (48) 30033-30038; January 28, 2020; <https://doi.org/10.1073/pnas.1907373117>.
  17. Lai, ZhiFei & Deng, Huifang. (2018). Medical Image Classification Based on Deep Features Extracted by Deep Model and Statistic Feature Fusion with Multilayer Perceptron. Computational Intelligence and Neuroscience. 2018. 1-13. 10.1155/2018/2061516.
  18. Najafabadi, M.M., Villanustre, F., Khoshgoftaar, T.M. et al. Deep learning applications and challenges in big data analytics. Journal of Big Data 2, 1 (2015). <https://doi.org/10.1186/s40537-014-0007-7>.
  19. Mikołajczyk and M. Grochowski, "Data augmentation for improving deep learning in image classification problem," 2018 International Interdisciplinary PhD Workshop (IIPHDW), 2018, pp. 117-122, doi: 10.1109/IIPHDW.2018.8388338.
  20. Shorten, C., Khoshgoftaar, T.M. A survey on Image Data Augmentation for Deep Learning. J Big Data 6, 60 (2019). <https://doi.org/10.1186/s40537-019-0197-0>
  21. Khan, Amjad & Atzori, Manfredo & Otálora Montenegro, Juan & Andrearczyk, Vincent & Müller, Henning. (2020). Generalizing Convolution Neural Networks on Stain Color Heterogeneous Data for Computational Pathology. 10.1117/12.2549718.
  22. Zarella MD, Yeoh C, Breen DE, Garcia FU (2017) An alternative reference space for H&E color normalization. PLoS ONE 12(3): e0174489. <https://doi.org/10.1371/journal.pone.0174489>
  23. Gurcan MN, Boucheron LE, Can A, Madabhushi [24] A, Rajpoot NM, Yener B. Histopathological image analysis: a review. IEEE Rev Biomed Eng. 2009;2:147-171. doi:10.1109/RBME.2009.2034865
  24. Hua Li, Shasha Zhuang, Deng-ao Li, Jumin Zhao, and Yanyun Ma. 2019. Benign and malignant classification of mammogram images based on deep learning. Biomedical Signal Processing and Control 51 (2019), 347–354.
  25. Marc Macenko, Marc Niethammer, James S Marron, David Borland, John T Woosley, Xiaojun Guan, Charles Schmitt, and Nancy E Thomas. 2009. A method for normalizing histology slides for quantitative analysis. In 2009 IEEE International Symposium on Biomedical Imaging: From Nano to Macro. IEEE, 1107–1110
  26. Liu, Jun-e & An, Fengping. (2020). Image Classification Algorithm Based on Deep Learning-Kernel Function. Scientific Programming. 2020. 1-14. 10.1155/2020/7607612.
  27. LeCun, Yann & Bengio, Y. & Hinton, Geoffrey. (2015). Deep Learning. Nature. 521. 436-44. 10.1038/nature14539.
  28. Chauhan, Rahul & Ghanshala, Kamal & Joshi, R.. (2018). Convolutional Neural Network (CNN) for Image Detection and Recognition. 278-282. 10.1109/ICSCCC.2018.8703316.
  29. O'Shea, Keiron & Nash, Ryan. (2015). An Introduction to Convolutional Neural Networks. ArXiv e-prints.
  30. Bengio, Y. & Lecun, Yann. (1997). Convolutional Networks for Images, Speech, and Time-Series.
  31. Yamashita, R., Nishio, M., Do, R.K.G. et al. Convolutional neural networks: an overview and application in radiology. Insights Imaging 9, 611–629 (2018). <https://doi.org/10.1007/s13244-018-0639-9>.
  32. Khan, Asifullah & Sohail, Anabia & Zahoora, Umme & Saeed, Aqsa. (2020). A Survey of the Recent Architectures of Deep Convolutional Neural Networks. Artificial Intelligence Review. 53. 10.1007/s10462-020-09825-6.
  33. Sze, Vivienne & Chen, Yu-Hsin & Yang, Tien-Ju & Emer, Joel. (2017). Efficient Processing of Deep Neural Networks: A Tutorial and Survey. Proceedings of the IEEE. 105. 10.1109/JPROC.2017.2761740.
  34. Agarap, A.F. (2018). Deep Learning using Rectified Linear Units (ReLU). ArXiv, abs/1803.08375.
  35. Krizhevsky, A. One weird trick for parallelizing convolutional neural networks. CoRR, abs/1404.5997, 2014. Krizhevsky, A., Sutskever, I., and Hinton, G. E. ImageNet classification with deep convolutional neural networks. In NIPS, pp. 1106–1114, 2012.

36. Simonyan, K. and Zisserman, A. Two-stream convolutional networks for action recognition in videos. CoRR, abs/1406.2199, 2014. Published in Proc. NIPS, 2014.
37. Zeiler, M. D. and Fergus, R. Visualizing and understanding convolutional networks. CoRR, abs/1311.2901, 2013. Published in Proc. ECCV, 2014.
38. Deng, J., Dong, W., Socher, R., Li, L.-J., Li, K., and Fei-Fei, L. Imagenet: A large-scale hierarchical image database. In Proc. CVPR, 2009.
39. Dean, J., Corrado, G., Monga, R., Chen, K., Devin, M., Mao, M., Ranzato, M., Senior, A., Tucker, P., Yang, K., Le, Q. V., and Ng, A. Y. Large scale distributed deep networks. In NIPS, pp. 1232–1240, 2012.
40. Russakovsky, O., Deng, J., Su, H., Krause, J., Satheesh, S., Ma, S., Huang, Z., Karpathy, A., Khosla, A., Bernstein, M., Berg, A. C., and Fei-Fei, L. ImageNet large scale visual recognition challenge. CoRR, abs/1409.0575, 2014.
41. Zisserman, Andrew. (2014). Very Deep Convolutional Networks for Large-Scale Image Recognition. arXiv 1409.1556.
42. He, Kaiming & Zhang, Xiangyu & Ren, Shaoqing & Sun, Jian. (2016). Deep Residual Learning for Image Recognition. 770-778. 10.1109/CVPR.2016.90.
43. Q. A. Al-Haija and A. Adebajo, "Breast Cancer Diagnosis in Histopathological Images Using ResNet-50 Convolutional Neural Network," 2020 IEEE International IOT, Electronics and Mechatronics Conference (IEMTRONICS), 2020, pp. 1-7, doi: 10.1109/IEMTRONICS51293.2020.9216455.
44. Szegedy, Christian & Vanhoucke, Vincent & Ioffe, Sergey & Shlens, Jon & Wojna, ZB. (2016). Rethinking the Inception Architecture for Computer Vision. 10.1109/CVPR.2016.308.
45. Xia, Xiaoling & Xu, Cui & Nan, Bing. (2017). Inception-v3 for flower classification. 783-787. 10.1109/ICIVC.2017.7984661.
46. Vesal, Sulaiman & Ravikumar, Nishant & Davari, Amirabbas & Ellmann, Stephan & Maier, Andreas. (2018). Classification of Breast Cancer Histology Images Using Transfer Learning. 10.1007/978-3-319-93000-8\_92.
47. Jannesari, Mahboubeh & Habibzadeh, Mehdi & Aboulkheyr, Hamidreza & Khosravi, Pegah & Elemento, Olivier & Totonchi, Mehdi & Hajirasouliha, Iman. (2018). Breast Cancer Histopathological Image Classification: A Deep Learning Approach. 2405-2412. 10.1109/BIBM.2018.8621307.